

**STRUCTURAL FEATURE OF AChE INHIBITOR  
HUPERZINE B IN NATURE AND IN THE BINDING  
SITE OF AChE: DENSITY FUNCTIONAL  
THEORY STUDY COMBINED  
WITH IR DETERMINATION**

XIAOMIN LUO, CHENG FENG, XIAO-JIAN TAN, CHANGHENG TAN,  
DAYUAN ZHU, JIANHUA SHEN, XIAOQIN HUANG, TONG LIU,  
KAIXIAN CHEN and HUALIANG JIANG<sup>\*,†</sup>  
*Center for Drug Discovery & Design and State Key Laboratory of Drug Research,  
Shanghai Institute of Materia Medica,  
Shanghai Institutes for Biological Sciences,  
Chinese Academy of Sciences,  
294 Taiyuan Road, Shanghai 200031, P. R. China  
\*jiang@iris3.simm.ac.cn  
\*hljiang@mail.shcnc.ac.cn*

WEILIANG ZHU and CHUM MOK PUAH<sup>†</sup>  
*Technology Centre for Life Sciences, School of Chemical & Life Sciences,  
Singapore Polytechnic, 500 Dover Road, Singapore 139651*

HAY DVIR, MICHAL HAREL and JOEL L. SUSSMAN<sup>†</sup>  
*Department of Structural Biology, Weizmann Institute of Science,  
76100 Rehovot, Israel*

ISRAEL SILMAN  
*Department of Neurobiology, Weizmann Institute of Science,  
76100 Rehovot, Israel*

Received 27 March 2002

Accepted 11 April 2002

Quantum chemical DFT-B3LYP/6-31G\* method and IR spectrometry have been used to investigate the natural and binding structures of Huperzine B (HupB) in order to better understand the interaction nature between acetylcholinesterase (AChE) and its inhibitor, with the view of designing new AChE inhibitors. The predicted and experimental results reveal that both the natural state and binding form of HupB adopt the chair conformation. Furthermore, the B3LYP/6-31G\* results suggest that structure S1 should be the dominant form of the two possible chair structures (S1 and S2, Fig. 2). The calculated results also show that the condensed ring structure composing of rings A, B and C is very rigid. Therefore, its flexibility does not need to be considered when we try to dock this structure to its target. Indeed, this supposition is confirmed by the excellent alignment of the binding structure produced from our recent X-ray crystallographic structure of the HupB-AChE complex with the B3LYP/6-31G\* predicted geometry. Among all the 111 predicted vibrational bands, the mode 110, which is resulted from the stretching of the bond N2–H and having the second highest frequency, is essential for the geometrical identification. The difference between our predicted strongest absorption band and experimental IR spectrum suggests

---

<sup>†</sup>Corresponding authors.

that a strong intermolecular interaction, which could be a hydrogen bond, exists in HupB crystal. The electrostatic potential surface of HupB derived from our B3LYP/6-31G\* CHelpG atomic charge suggests a mechanism of how HupB would interact with its target. In addition, the good agreement between predicted vibrational bands (scaled by a factor of 0.96) and experimental result shows that B3LYP/6-31G\* is a good tool for studying such kind of natural compound.

*Keywords:* Density-functional theory; conformation; electrostatic potential surface; vibrational spectrum.

## 1. Introduction

Hydrolyzing the neural transmitter acetylcholine (ACh), acetylcholinesterase (AChE) plays a key role in both central and peripheral nervous systems in the transmission of action potentials across nerve-nerve and neuromuscular synapses.<sup>1</sup> Studies on AChE inhibitors have shown that the reversible inhibitors of AChE can make their ways into the central nervous system, indicating that these inhibitors may be useful in allaying the symptoms that interrelate to the unusually high activity of AChE.<sup>2-7</sup>

With a view to develop new inhibitors of AChE, we have designed some new derivatives of huperzine (HupA) based on the X-ray crystal structure of AChE-HupA complex.<sup>8</sup> However, all the assayed activities of our designed compounds to AChE did not show the expected activities.<sup>9</sup> Other research groups also reported similar findings.<sup>10,11</sup> Therefore, it is of paramount importance to investigate the interaction mechanism in greater details between AChE and its inhibitors, so that we can understand how inhibitors interact with AChE. This interaction mechanism will be undoubtedly helpful in designing new potent inhibitors of AChE. To achieve this purpose, we have been performing a series of studies based on both theoretical and experimental methods.<sup>8,12-14</sup> Here we report our recent theoretical finding on Huperzine B (HupB) conformations in its natural state and in its binding state with AChE.

Like HupA, HupB is also an alkaloid isolated from the Chinese Herb *Huperzia Serrata Thunb.*<sup>15</sup> Its skeleton is composed of four condensed ring structure (rings A, B, C and D, Fig. 1). Pharmacological studies have demonstrated that HupB is capable of inhibiting AChE with low toxicity.<sup>15,16</sup> Hence studies on its structural characteristics and on its binding nature to AChE are essential in better understanding the interaction mechanism of AChE and its inhibitors, furthermore in designing new AChE inhibitors which

can be used to treat diseases that are believed to be associated with cholinergic insufficiency such as, Alzheimer's Disease (AD) and myasthenia.

To the best of our knowledge, the X-ray crystallographic structure and IR spectrum of HupB have not been reported. Moreover, there is paucity of data on its molecular structure and vibration mode analysis. The assignment of absorption bands of infrared spectrum (IR) for complicated natural product poses a challenge to structural chemists. Until recently, quantum chemistry calculation on complicated natural products is hampered by the lack of huge computer resources. However, following the rapid advance in computer hardware, density functional theory (DFT) has been recognized as an efficient computational tool for studying molecular properties.<sup>17,18</sup> Indeed our previous quantum chemical calculations have shown that DFT at B3LYP/6-31G\* level is a good approach

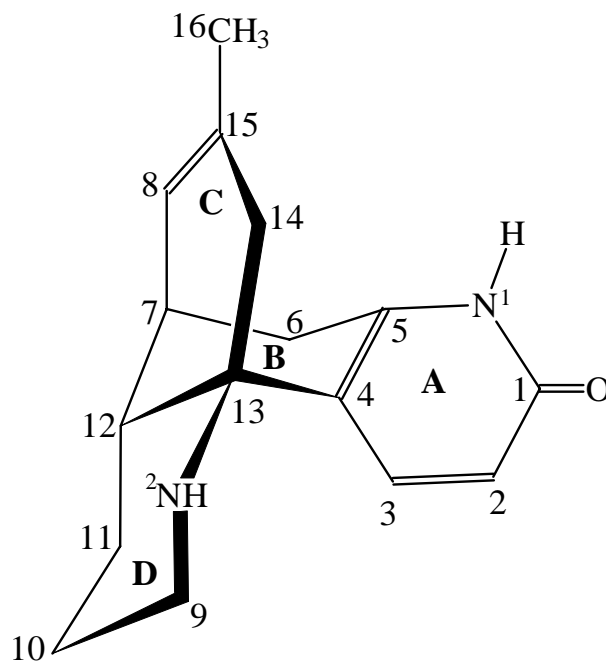


Fig. 1. The structure of Huperzine B.

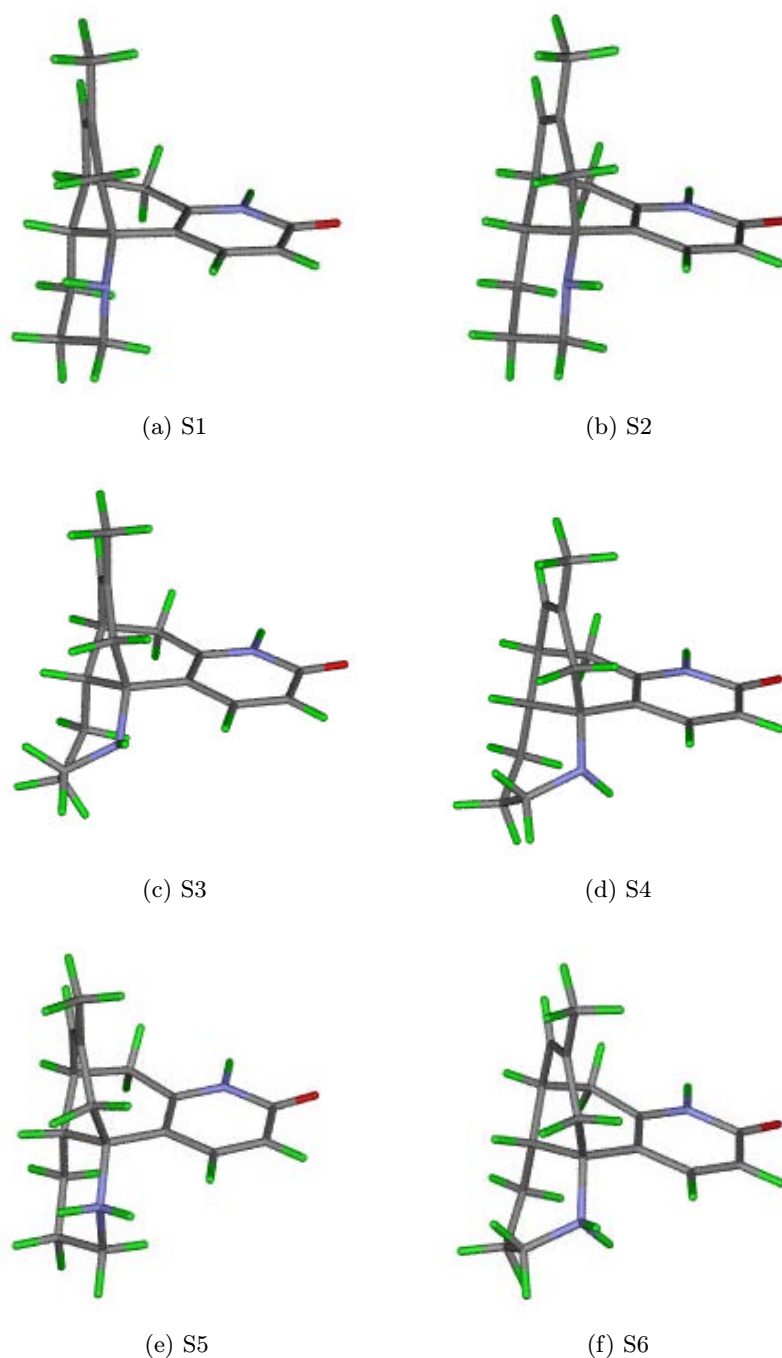


Fig. 2. The six optimized HupB structures. Picture was made with WebLib<sup>TM25</sup> and rendered in POV-ray<sup>©26</sup>

for studying molecular properties, such as geometry, thermodynamic parameter and IR spectrum.<sup>19,20</sup> Therefore, B3LYP/6-31G\* method is used throughout this study.

## 2. Computational and Experimental Details

Six different possible initial structures of HupB were constructed with molecular modeling software

Sybyl 6.5.<sup>21</sup> They can be divided into two types: free HupB (S1 to S4) [Figs. 2(a) to 2(d)] and protonated HupB (S5 and S6) [Figs. 2(e) and 2(f)] in view of the protonation of HupB under physiological condition. After primarily optimization by use of AM1<sup>22</sup> semiempirical quantum chemistry module encoded in Sybyl, these six structures of HupB were subjected to full optimization employing the DFT method B3LYP<sup>23</sup> at 6-31G\* level of theory. Based on the optimized geometries, frequency calculations were carried out at the same levels of B3LYP so as to verify the reasonability of the optimized structures, and to determine enthalpies and entropies and thus, the proton affinity of HupB. All Molecular Mechanics calculations were performed on SGI Indigo II workstation with Sybyl 6.5.<sup>21</sup> All the Quantum Chemical calculations were carried out with Gaussian 98 program<sup>24</sup> on Power Challenge R10000 and Origin 2000 computers.

The IR spectrum of HupB is recorded on an IR-901(H-14/KBR) instrument.

### 3. Results and Discussion

#### 3.1. Predicted geometry

Chemical intuition suggests that the extra hexacyclic ring of HupB can adopt either chair or boat conformation. In order to address the conformational features of HupB in the AChE binding site and in nature, we performed a quantum chemistry calculation for the possible conformations of HupB, in particular for the conformations of the extra ring (ring D; Fig. 1), in both the neutral and protonated states by use of density-functional theory method B3LYP<sup>23</sup> at the 6-31G\* basis set level. The calculated results are presented in Table 1 and Fig. 2. For the neutral state, there are two options to add the hydrogen atom onto the secondary amine nitrogen atom in the extra ring, i.e., through axial (*a*-bond) or equatorial (*e*-bond) orientation. This would result in neutral state having four possible conformations or structures (S1–S4; Fig. 2). The chair or boat conformation of the protonated-state of HupB has only one option for the orientations of the two hydrogen atoms attached onto the secondary amine nitrogen (S5 and S6; Fig. 2). Among the four neutral state HupB structures, the energies of boat forms are higher than that of chair forms by 5.4–7.5 kcal mol<sup>-1</sup>, suggesting that

the chair form is energetically the favorable structure. Table 1 shows that S1 has the lowest energy amongst the four free HupB structures, suggesting that it is the most probable structure existing in nature. Table 1 also shows that the energy difference between S2 and S1 is only 0.982 kcal mol<sup>-1</sup>, suggesting that these two conformations could coexist in nature. Indeed, according to the principle of Boltzmann's distribution, the distribution of these four conformations is S1 : S2 : S3 : S4 = 1 : 0.19 : 3.3 × 10<sup>-6</sup> : 2.2 × 10<sup>-5</sup>. These data clearly show that the chair form is the dominant structure in its neutral state. It is a fact that an amino group could change its configuration in aqueous solution by means of protonation and deprotonation. Since the difference between S1 and S2 lies in only the orientation of amino hydrogen, we think that HupB can adjust its orientation of the hydrogen atom attached to N2 in order to fit either the environmental or enzyme requirement.

Similar to the neutral state, the protonated HupB with chair form conformation was also found to be more stable than that with boat conformation by 4.9 kcal mol<sup>-1</sup>. The Boltzmann's distribution value of S5 : S6 was found to be 1 : 2.5 × 10<sup>-4</sup>, suggesting that the chair form of protonated HupB is most likely the dominated candidate.

In order to understand the effect of the structure of ring D to the other part of HupB, we align all the heavy atoms of rings A, B and C of all optimized structures. Figure 3 depicts the alignment results. Between S1 and other five structures, we found the alignment RMS values to range from 0.007 to 0.059. Both the RMS value and Fig. 3 showed that the condensed ring structure composed of A, B and C is very rigid and remains stable irrespective of what form and conformation that ring D adopts. We infer from these results that ring D does not significantly affect the geometry of the other part of this molecule. Indeed, this conclusion is consistent with our previous finding on quantum chemical calculations for Huperzine A.<sup>19</sup> Therefore, when we dock Huperzine analogues, either Huperzine A or HupB, into the active site of its receptor, we do not need to take into account the flexibility of the condensed ring structure of A, B and C.

Figure 3 also shows that structure S2 can be aligned perfectly to S1 with the exception of the –NH– group of ring D. The distance between N2 and the H attached to C3 in structure S1 is shorter than

Table 1. The energies for the conformations of HupB and the thermodynamic parameters for the proton affinity of HupB<sup>a</sup>.

Structure	(a) Energies and thermodynamic parameters for the isolated structures of different conformations							
	S1	S2	S3	S4	S5	S6	H <sub>2</sub> O	OH <sup>-</sup>
$E_t^b$	-806.48120	-806.47964	-806.46929	-806.471069	-806.86340	-806.85556	-75.97397	-75.72077
$\Delta E_{\text{rel}}^c$	0.0	0.982	7.476	6.367	-239.830	-234.907		
$E_{\text{thermal}}^d$	222.481	222.421	222.447	222.459	231.833	231.827	14.160	6.366
$S^e$	120.252	120.484	122.362	121.532	121.354	122.842	46.683	41.253
	(b) Free energies for the protonation and protonation affinities of HupB							
	S1 → S5	S1 → S6	S2 → S5	S2 → S6	S3 → S5	S3 → S6	S4 → S5	S4 → S6
$\Delta G_{\text{abs}}^f$	-78.0987	-73.6252	-78.9516	-74.4782	-84.9118	-80.4383	-84.0617	-79.5883
$\Delta G_{\text{aff}}^g$	-231.397	-226.923	-232.25	-227.776	-238.21	-233.736	-237.36	-232.886

<sup>a</sup> All the energies were calculated in the gas phase using B3LYP/6-31G\*. The various structure conformations correspond to those presented in Fig. 2. The free energies correspond to the energy required for the transition from one conformation to another in two ways: abstract and affinity.

<sup>b</sup>  $E_t$ : total energy (a.u.).

<sup>c</sup>  $\Delta E_{\text{rel}}$ : relative energy (kcal mol<sup>-1</sup>).

<sup>d</sup>  $E_{\text{thermal}}$ : thermal energy (kcal mol<sup>-1</sup>).

<sup>e</sup> S: entropy (cal mol<sup>-1</sup> K<sup>-1</sup>).

<sup>f</sup>  $\Delta G_{\text{abs}}$ : the free energy change (kcal mol<sup>-1</sup>) of the virtual reaction of HupB + H<sub>2</sub>O → HupBH<sup>+</sup> + OH<sup>-</sup>. The calculation method is as follows,

$$\begin{aligned}\Delta E_{\text{abs}} &= E_t(\text{HupBH}^+) + E_t(\text{OH}^-) - E_t(\text{HupB}) - E_t(\text{H}_2\text{O}) \\ \Delta E_{\text{therm}} &= E_{\text{therm}}(\text{HupBH}^+) + E_{\text{therm}}(\text{OH}^-) - E_{\text{therm}}(\text{HupB}) - E_{\text{therm}}(\text{H}_2\text{O}) \\ \Delta S_{\text{abs}} &= S(\text{HupBH}^+) + S(\text{OH}^-) - S(\text{HupB}) - S(\text{H}_2\text{O}) \\ \Delta H_{\text{abs}} &= \Delta E_{\text{abs}} + \Delta E_{\text{therm}} + \Delta(PV) \\ \Delta G_{\text{abs}} &= \Delta H_{\text{abs}} - T\Delta S_{\text{abs}}\end{aligned}$$

<sup>g</sup>  $\Delta G_{\text{aff}}$ : the proton affinity (kcal mol<sup>-1</sup>) of HupB + H<sup>+</sup> → HupBH<sup>+</sup>. The calculation method is the same as described above.

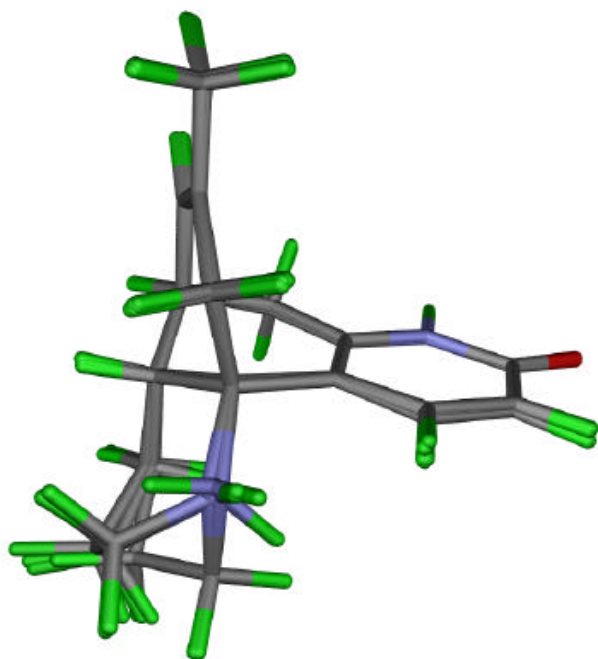


Fig. 3. The alignment of six optimized HupB structures. Picture was made with WebLib<sup>TM</sup><sup>25</sup> and rendered in POV-ray<sup>©</sup><sup>26</sup>

that in S2 by 0.20 Å (2.713 Å–2.513 Å). The longer distance in S2 could arise from the repulsion between the two positively charged hydrogen atoms attached to N2 and C3 [Figs. 1(d) and 2(b)], respectively. This repulsion could be one of the reasons why the energy of structure S2 is slightly higher than that of S1 (Table 1).

As an example, we summarized the optimized geometrical parameters of S1 in Table 2 so as to investigate the structural characteristics of HupB molecule. The dihedral in Table 2 shows that all the atoms of pyridone are on a plane in which the deviation is not more than 1.0 degrees. On the other hand, the longest C–C bond in structure S1 belongs to C12–C13, which measures 1.554 Å. This could arise from the special position of this bond that utilized as a junction between rings B and D (Fig. 1).

### 3.2. The binding conformation of HupB

Based on the discussion above, we know that the condensed structures of rings A, B and C are very rigid. Besides the chair form being the dominant form existing in the gas phase, it is also most likely to be the binding form of HupB interacting to AChE.

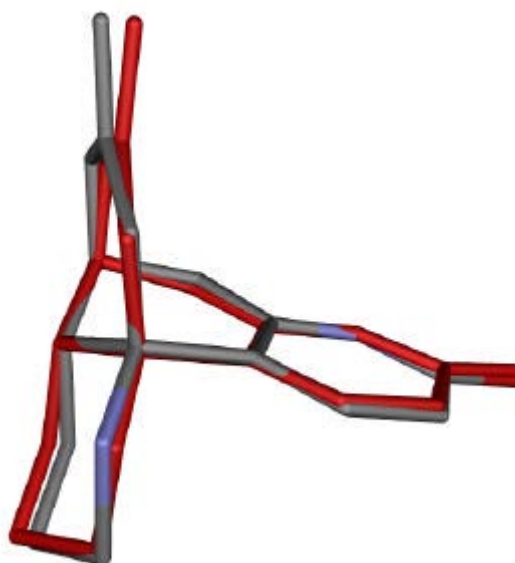


Fig. 4. The alignment of HupB in the *x*-ray crystal structure of *Tc*AChE-HupB complex (colored by atom type) with S1 predicted by B3LYP/6-31G\* (colored by red). Picture was made with WebLib<sup>TM</sup><sup>25</sup> and rendered in POV-ray<sup>©</sup><sup>26</sup>

Indeed, this supposition is consistent with our recently determined X-ray crystal structure of AChE-HupB complex.<sup>27</sup> Figure 4 depicts the alignment diagram of B3LYP/6-31G\* predicted geometry and the binding configuration extracted from our X-ray crystal structure of HupB-AChE complex. It is clear that the skeleton of HupB does not pose a significant change in the comparison of predicted one, suggesting once again that the condensed ring structure is very rigid.

### 3.3. Protonation affinity

Like the amino group of HupA, the secondary amine group may be protonated (positively charged) at the pH of the crystallization conditions (pH = 5.6).<sup>8,27</sup> However, most of the macromolecule X-ray structures cannot prove this, because the electron density map is of low resolution and therefore unable to resolve short distances such as N–H bond. We therefore calculated the free energy changes of HupB when it abstracts a hydrogen atom from a water molecule or a free proton from solution (protonation affinity), for all the four possible conformations using the total energies, thermal energies and entropies (Table 1). The computational method is shown in the footnote of Table 1.

Table 2. The optimized geometrical parameters.

Bond Length	Å	Bond Angle	Degree	Torsion	Degree
C1-C2	1.4496	N1-C1-C2	112.5	C1-C2-C3-C4	0.2
C2-C3	1.3648	C1-C2-C3	121.4	C2-C3-C4-C5	-0.9
C3-C4	1.4319	C2-C3-C4	122.5	C3-C4-C5-N1	1.0
C4-C5	1.3734	C3-C4-C5	117.3	C4-C5-N1-C1	-0.4
C5-N1	1.3708	C4-C5-N1	119.4	C3-C4-C5-C6	-179.7
C5-C6	1.5079	C5-N1-C1	126.8	C4-C5-C6-C7	13.6
C6-C7	1.5462	C4-C5-C6	124.1	C5-C6-C7-C8	76.2
C7-C8	1.5137	C5-C6-C7	111.2	C6-C7-C8-C15	-99.0
C8-C15	1.3396	C6-C7-C8	110.1	C7-C8-C15-C14	-1.3
C14-C15	1.5132	C7-C8-C15	123.9	C8-C15-C14-C13	12.7
C13-C14	1.5493	C8-C15-C14	121.5	C15-C14-C13-C12	-44.5
C12-C13	1.5536	C13-C14-C15	113.9	C14-C13-C12-C7	66.3
C7-C12	1.5418	C12-C13-C14	107.9	C13-C12-C7-C8	-54.8
C4-C13	1.5336	C7-C12-C13	107.9	C4-C13-C12-C11	74.1
C11-C12	1.5386	C8-C7-C12	110.0	C3-C4-C13-N2	-35.8
C10-C11	1.5351	C11-C12-C13	112.6	C4-C13-N2-C9	-74.4
C9-C10	1.5363	C10-C11-C12	111.0	C13-N2-C9-C10	-52.6
C9-N2	1.4687	C9-C10-C11	110.0	N2-C9-C10-C11	55.0
C13-N2	1.4777	N2-C9-C10	113.6	C7-C8-C15-C16	179.3
C1-O	1.2286	C9-N2-C13	114.7	C3-C2-C1-O	-179.8
C15-C16	1.5066	N2-C13-C12	113.0	C4-C13-N2-H	163.6

The free energy of abstracting hydrogen from water ranges from  $-73$  to  $-85$  kcal mol $^{-1}$ , and the protonation affinity ranges from  $-226$  to  $-238$  kcal mol $^{-1}$  at B3LYP/6-31G\* level of theory. This indicates that even in neutral aqueous solution, the protonation of HupB is thermodynamically favorable. Based on this, we also assume that HupB binds to AChE mainly in its protonated form. B3LYP/6-31G\* calculation indicated that the protonation of HupB have decreased the energy gap between its chair conformation and boat conformation. But still, the chair conformation is 4.9 kcal mol $^{-1}$  more stable than the boat one (Table 1). The X-ray electron density map<sup>27</sup> and the DFT quantum chemistry calculation show that the preferred conformation of HupB in the enzyme active site, gas phase and in solution is the same. These results may account for the efficient inhibition of AChE by HupB, because there is no entropy loss for HupB binding to AChE.

### 3.4. Electrostatic potential surface

Figure 5 depicts the electrostatic potentials of S5 and

S6 conformations on their Van der Waal's surface derived from our B3LYP/6-31G\* CHelpG charges.<sup>28</sup> It appears that most of the surface of HupB is positively charged, indicating that a site with rich negative charge is favorable for the binding of HupB. This is in agreement with our earlier study in which X-ray study on AChE revealed that its active site is lined by an array of conserved aromatic side chains.<sup>8,29</sup> Incidentally these aromatic rings are rich in  $\pi$  electron, whereby they should bind well with the positively charged surface of HupB. Figure 5 also shows two sites that are obviously negatively charged, in which they are associated with atoms O and N2. Hence, these negative sites should be as far away as possible from the aromatic side chains. These results are also in accordance with our X-ray crystallographic results on the complex between HupB and AChE. In this complex, the oxygen of C=O bond of HupB is likely to form hydrogen bonds with a water molecule and with the residue TYR130. Meanwhile, the N2 part of HupB is directed towards the gate of AChE active site.<sup>27</sup> From Fig. 5, we can see that the surface of rings C and D of conformation S5 hold a more positive charge than that of

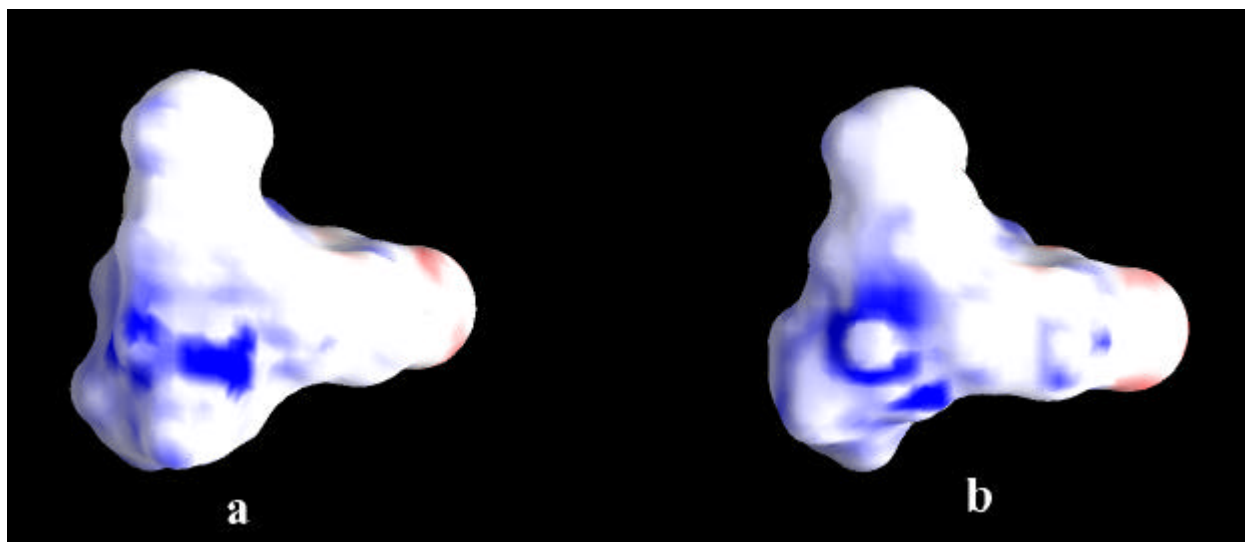


Fig. 5. Electrostatic potential surfaces of the two conformations of the protonated HupB, S1(a) and S2(b), derived from B3LYP/6-31G\* CHelpG charge.<sup>28</sup> The electrostatic potentials were generated with the program GRASP.<sup>30</sup> The orientations for S1 and S2 are the same as that in Fig. 2.

conformation S6; and ring A of S5 holds a more negative charge than that of S6. In addition, the dipole moment of S5 (9.6 D) is larger than that of S6 (9.5 D). All these facts indicate that S1 is beneficial for binding with AChE. The electrostatic potential calculation for S5 and S6 demonstrates further that the protonated HupB binding with AChE adopting the chair conformation.

### 3.5. *Vibrational spectrum*

The calculated vibrational spectra have no imaginary frequency, implying that the optimized geometries are located at minimum points of the potential surface of HupB. In general, there are 111 and 114 vibration modes for each geometry of free HupB and protonized HupB, respectively. The strongest absorption band for free HupB is mode 91 with an intensity of  $\sim 680 \text{ KM mol}^{-1}$ . It has been known that, because of some reasons such as anharmonic effect, vibrational intensity could not be estimated very accurately by use of current quantum chemistry computational methods. Hence, we are more likely to pay close attention to the calculated frequency rather than its intensity in the following discussion. Since the crystal of free HupB, rather than protonated HupB, is used in our IR spectral determination, we will confine our

discussion on the former. Normally there will be a systematic error between calculated and experimental spectra, which can be adjusted by a scaling factor.<sup>31,32</sup> The typical value of this scaling factor ranges from 0.7 to 0.9 for Hartree–Fock method. Compared with experimental IR spectrum, we note that the scaling factor for our predicted vibrational bands is 0.96. Figure 6 depicts the scaled vibrational bands of structure S1 together with our experimental IR spectrum. It is clear that the scaled predicted bands are in agreement with experimental data. This result, taking into account our previous result,<sup>19,20</sup> shows that we can use B3LYP/6-31G\* method to predict the vibrational spectrum of complicated natural product with great accuracy than the Hartree–Fock method.

#### 3.5.1. *The assignment of vibrational band*

Experimental IR spectrum shows that there are about 22 absorption peaks ranging from  $500 \text{ cm}^{-1}$  to  $3500 \text{ cm}^{-1}$ . In order to assign these bands as well as to verify our prediction that the natural configuration of HupB is structure S1, we perform a normal mode analysis on the predicted bands of structure S1. Table 3 lists both the normal mode analysis and experimental results.

Table 3. Predicted and experimental IR.

Mode No.	Normal Mode Analysis Result				Experimental Result	
	Freq <sup>a</sup>	Freq <sup>b</sup>	Inten <sup>c</sup>	Assignment Result	Freq	Transm <sup>d</sup>
27	653	627	11.7	breathing of rings A, B, C & D	625	82
28	686	659	4.1	out of plane of the H of N1-H, breathing of rings A, B, C & D	653	60
29	713	684	26.3	out of plane of the H of N1-H	684	78
31	758	728	46.0	rocking of the H of N2-H	730	70
36	853	819	34.8	breathing of rings A, B and C, rocking of Hs of A, B, C & D	(816)	88
38	883	848	16.1	rocking of the Hs of rings B, C and D	840	53
42	941	903	10.5	breathing of rings A, B, C & D, rocking of Hs of A, B, C & D	916	58
53	1118	1073	18.8	rocking of Hs of rings A, B, C & D		
55	1144	1098	49.5	rocking of Hs of rings A, B, C & D	1095	67
59	1203	1155	14.9	rocking of the Hs of N1-H and C3-H, rocking of H-C6-H	1154	72
61	1229	1180	7.1	rocking of the Hs of rings B, C & D	1178	72
66	1306	1254	22.8	breathing of rings A, B, C & D	1256	81
67	1336	1283	1.6	rocking of the Hs of rings B, C & D	1280	71
70	1369	1314	5.1	rocking of the Hs of rings B & D	1309	60
76	1415	1358	1.2	rocking of the hydrogen of C11-H and C12-H	1365	73
79	1477	1418	19.7	stretching of N1-C5, bending of H-N1-C5	1417	61
80	1499	1439	3.7	rocking of the Hs of C14 and N2	1429	47
86	1523	1462	11.7	bending of the Hs of N2 and C10	1452	43
88	1604	1540	77.5	stretching of C2-C3 and C4-C5	1546	58
89	1670	1603	35.7	stretching of C2-C3 and C4-C5	1604	28
91	1788	1716	680.0	stretching of C1=O and bending of N1-C1-C2	1666	2
92	2985	2866	38.2	stretching of C14-H	2864	38
98	3038	2916	65.7	stretching of the Hs of C6-H, C7-H and C11-H	2914	32
106	3124	2999	18.3	stretching of the Hs of C16-H		
107	3149	3023	36.3	stretching of the Hs of C8-H		
108	3205	3077	1.6	stretching of the Hs of C3-H & H-C2	3080	67
109	3231	3102	7.0	stretching of the Hs of C2-H		
110	3477	3338	2.3	stretching of the Hs of N2-H	3331	85
111	3577	3434	32.7	stretching of the Hs of N1-H	3428	87

<sup>a</sup> Frequency before scaling.

<sup>b</sup> Frequency scaled with a factor of 0.96.

<sup>c</sup> Predicted intensity.

<sup>d</sup> Recorded IR transmission.

• **The bands with frequency higher than 2500 cm<sup>-1</sup>**

Normal mode analysis on all these 20 bands, from mode 92 to mode 111, shows that they arise from the stretching of H-C or H-N bonds (Table 3). Among which, mode 92 to mode 106 (2866 cm<sup>-1</sup> to 2999 cm<sup>-1</sup>) correspond to the stretching of H-C bonds. Our recorded IR spectrum shows a broad and strong absorption ranging from 2800 to 3000 cm<sup>-1</sup>. For example, mode 92 (2866 cm<sup>-1</sup>) belongs to the

stretching of C14-H bond, which should correspond to the band 2864 cm<sup>-1</sup> in our experimental spectrum (Table 3). Normal mode analysis reveals that mode 98 (2916 cm<sup>-1</sup>) results from the stretching of C6-H, C7-H and C11-H bonds. Corresponding to this predicted band, there is a peak at 2914 cm<sup>-1</sup> in the recorded spectrum (Table 3 and Fig. 6).

Modes 107 (3023 cm<sup>-1</sup>), 108 (3077 cm<sup>-1</sup>) and 109 (3102 cm<sup>-1</sup>) belong to the stretching of bonds C8-H, C3-H and C2-H, respectively (Table 3). For these

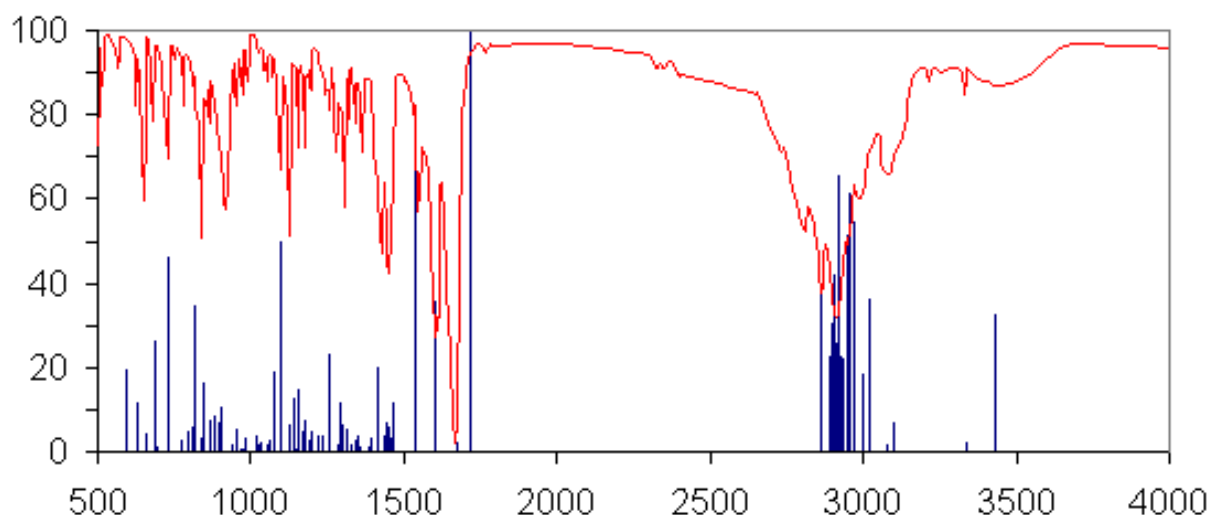


Fig. 6. The predicted and experimental spectra of HupB. Lines stand for the predicted bands at B3LYP/6-31G\* level, curve is the recorded IR spectrum.

three carbon atoms are  $sp^2$  hybridization, their corresponding frequencies should be higher than that relevant to  $sp^3$  carbon atom. Moreover, the predicted intensities of modes 108 and 109 are rather weak. Indeed, these calculated results are consistent with the experimental data, in which a broad and weak peak located at  $\sim 3087\text{ cm}^{-1}$  was recorded (Fig. 6).

The predicted highest frequency, mode 111 ( $3434\text{ cm}^{-1}$ ) belongs to the stretching of the bond N1-H, which might be assigned to the recorded band with the frequency  $3428\text{ cm}^{-1}$ . The second highest frequency, mode 110 ( $3338\text{ cm}^{-1}$ ) is related to the stretching of bond N2-H. Experimental result suggests a band located at  $3331\text{ cm}^{-1}$  (Fig. 6). It is notable that this band is related to the hydrogen atom attached to N2 (Fig. 1). More detailed discussion is shown in the next sub-subsection on “The Comparison of the Characteristic Bands Predicted Based on Different structures”.

- ***The bands with frequencies from 1700 to  $1350\text{ cm}^{-1}$ .***

Normal mode analysis on the predicted strongest absorption band, mode 91 ( $1788\text{ cm}^{-1}$ ,  $680.0\text{ KM mol}^{-1}$ ) reveals that this band is a result of coupling between the stretching of the bond C=O and the bending of N1-C1-C2. However, our recorded spectrum suggests a strong absorption located at  $1666\text{ cm}^{-1}$ , which turns

out to be lower than the predicted one (Table 3 and Fig. 6). This result suggests that the strength of C=O bond in crystal is weaker than that in single molecule state. We postulate that, as shown in the case of the crystal structure of HupA,<sup>33</sup> there should be a strong intermolecular interaction, such as hydrogen bond, possibly related to this C=O bond. This interaction weakens the strength of C=O bond in crystal, and results in a vibrational shift towards low frequency.

Mode 89 ( $1603\text{ cm}^{-1}$ ) belongs mainly to the stretching of C2-C3 and C4-C5 bonds, which correspond to the band of  $1604\text{ cm}^{-1}$  in our recorded spectrum. Normal mode analysis result suggests that mode 88 ( $1540\text{ cm}^{-1}$ ) is also caused by the stretching of C2-C3 and C4-C5 bonds, corresponding to the band of  $1546\text{ cm}^{-1}$  in the experimental result (Table 3). Mode 86 ( $1462\text{ cm}^{-1}$ ) arises from the coupling of the rocking action of the hydrogen of N2-H and H-C10-H. This seems to tally with the observed band at  $1452\text{ cm}^{-1}$  found in our IR spectrum. The recorded peak at  $1429\text{ cm}^{-1}$  with a shoulder at  $1417\text{ cm}^{-1}$  should correspond to modes 80 and 79 (Fig. 6, Table 3). The predicted band, mode 76 ( $1358\text{ cm}^{-1}$ ), corresponding to the experimental band  $1365\text{ cm}^{-1}$ , could be due to the coupling of the rocking actions between the hydrogen of C11-H and C12-H (Table 3).

• *The bands with frequency under  $1350\text{ cm}^{-1}$*

It is difficult for chemist to assign bands in this region. As a matter of fact, normal mode analysis on this region also shows that most of these bands are a result of coupling action of several different vibrations. The exceptions are modes 29 and 31, which are related to the rocking of the hydrogen atoms of N1-H and N2-H, respectively (Table 3).

3.5.2. *The comparison of the characteristic bands predicted based on different structures*

All the 4 predicted spectra of free HupB have a similar highest frequency at  $\sim 3577 \pm 1\text{ cm}^{-1}$  (mode 111, unscaled), as well as the strongest absorption band at  $\sim 1788 \pm 1\text{ cm}^{-1}$  (mode 91, unscaled). They are due to the vibrations of N1-H and C1=O, respectively. We have shown that ring D does not obviously affect ring A, which means that these two bands should be similar to each other among these four structures of free HupB. We have discussed that the difference between structures S1 and S2 is only due to the orientation of the hydrogen atom attached to N2. Hence, mode 110, which is caused by the stretching of N2-H bond, is an important band to identify in these two structures. Our calculations show that the wave number of this mode for S2 is higher than that for S1 by  $23\text{ cm}^{-1}$ . If S2 is the prominent structure, there should be a band located at  $3360\text{ cm}^{-1}$  (scaled). On the contrary, our experimental spectrum does not reveal such a band in HupB IR spectrum (Fig. 6). Similar argument applies to the boat structures. We found that mode 110 of boat structures tend to have higher frequencies by  $\sim 20\text{ cm}^{-1}$  compared to S1's. Hence, mode 110 proved to be useful for identifying the structure of free HupB. All these results demonstrate that S1 is the natural structure of HupB.

#### 4. Conclusion

Our B3LYP/6-31G\* calculations and experimental IR spectrum reveal that HupB always adopts the chair configuration either in its natural form or as a complex with AChE irrespective of which state it exists as, free or protonated. Furthermore, the calculation results suggest that structure S1 has a dominant distribution in two possible chair forms, viz. S1 and S2.

All the predicted structures also show that condensed ring structure made up of rings A, B and C is very rigid which mean that we do not have to take into consideration its flexibility in our docking calculations. Indeed this result is confirmed by its binding structure from our recent X-ray crystallographic results in which all bonds could be aligned quite well to the predicted geometry (Fig. 4). Further evidence came from our normal mode analysis on all 111 predicted vibration modes in supporting S1 as the most probable structure of HupB. This same normal mode analysis also highlighted that the second highest frequency (mode 110) is very useful for identifying the structure of HupB due to the stretching of N2-H bond. Furthermore, almost all of the experimental absorption bands could be accounted for and assigned to their vibration modes. The obvious shifting of the stretching of C=O bond in our recorded HupB spectrum towards low frequency in comparison with the predicted bands suggested the existence of a strong intermolecular interaction in HupB crystal. The excellent alignment of the predicted bands scaled by a factor of 0.96 to experimental IR spectrum suggests that B3LYP/6-31G\* method is a good tool for studying such kind of complicated natural compound. The electrostatic potential surface of HupB, taken into consideration with our recent X-ray structural studies of its complex with AChE, reveals a clearer picture of how HupB interacts with its targeted site. All these results will enhance further investigation of Huperzine analogues interacting with AChE leading to better development of potent AChE inhibitor/drugs.

#### Acknowledgments

We gratefully acknowledge financial support from the National Natural Science Foundation of China (Grant 29725203), the "863" High-Tech Program of China (Grant 863-103-04-01), the State Key Program of Basic Research of China (Grant 1998051115). This work was also supported by the U.S. Army Medical and Material Command under Contract No. DAMD17-97-2-7022, the EU 4th Framework Program in Biotechnology, the Kimmelman Center for Biomolecular Structure and Assembly (Rehovot, Israel), and the Dana Foundation. The generous support of Mrs. Tania Friedman is gratefully acknowledged too. I. S. is Bernstein-Mason Professor of Neurochemistry.

The quantum chemistry calculations were performed on Power Challenge R10000 at The Network Information Center, Chinese Academy of Sciences, Beijing, P. R. China and Origin 2000 at Weizmann Institute of Science, Rehovot, Israel.

## References

1. D.M. Quinn, *Chem. Rev.* **87**, 955–979 (1987).
2. S.B. Dunnett and H.C. Fibiger, *Prog. Brain Res.* **98**, 413–420 (1993).
3. S. Laganière, J. Corey, X.C. Tang, E. Wülfert and I. Hanin, *Neuropharmacology* **30**, 763–768 (1991).
4. W.K. Summers, V. Majovski, G.M. Marsh, K. Tachiki and A. Kling, *N. Engl. J. Med.* **315**, 1241–1245 (1986).
5. S.L. Nightingale, *J. Amer. Med. Assoc.* **277**, 10 (1997).
6. M. Weinstock, M. Razin, M. Chorev and A. Enz, *J. Neur. Trans. Suppl.* **43**, 219–225 (1994).
7. D.S. Knopman, *Neurology* **50**, 1203–1205 (1998).
8. M.L. Raves, M. Harel, Y.P. Pang, I. Silman, A.P. Kozikowski and J.L. Sussman, *Nat. Struct. Biol.* **4**, 57–63 (1997).
9. F.X. Zeng, H.L. Jiang, X.C. Tang, K.X. Chen and R.Y. Ji, *Bioorg. Med. Chem. Lett.* **8**, 1661–1664 (1998).
10. S. Kaneko, N. Nakajima, M. Shikano, T. Katoh and S. Terashima, *Bioorg. Med. Chem. Lett.* **6**, 1927–1930 (1996).
11. S. Kaneko, M. Shikano, T. Katoh and S. Terashima, *Synlett.* **5**, 447–448 (1997).
12. W.L. Zhu, H.L. Jiang, C.M. Puah, X.J. Tan, K.X. Chen, Y. Cao and R.Y. Ji, *J. Chem. Soc. Perkin Trans. II* **11**, 2615–2622 (1999).
13. W.L. Zhu, X.J. Tan, C.M. Puah, J.D. Gu, H.L. Jiang, K.X. Chen, C.E. Felder, I. Silman and J.L. Sussman, *J. Phys. Chem.* **A104**, 9573–9580 (2000).
14. I. Silman, M. Harel, P. Axelsen, M. Raves and J.L. Sussman, *Biochem. Soc. Trans.* **22**, 745–749 (1994).
15. J.S. Liu, C.M. Yu, Y.Z. Zhu, Y.Y. Han, F.W. Wu, B.F. Qi and Y.L. Zhu, *Can. J. Chem.* **64**, 837–839 (1986).
16. H. Xu and X.C. Tang, *Acta Pharmacol. Sin.* **8**, 18–22 (1987).
17. R.G. Parr and Y. Yang, *Density-Functional Theory of Atoms and Molecules* (Oxford University Press, Oxford, U.K., 1989).
18. D.P. Chong (ed.), “Recent advances in density functional methods,” in *Recent Advances in Computational Chemistry*, Vol. 1, (World Scientific, Singapore, 1997).
19. W.L. Zhu, H.L. Jiang, J.D. Gu, J.Z. Chen, J.K. Shen, K.X. Chen, R.Y. Ji and Y. Cao, *J. Mol. Str. (THEOCHEM)* **488**, 21–28 (1999).
20. W.L. Zhu, C.K. Puah, X.J. Tan, H.L. Jiang, K.X. Chen and R.Y. Ji, *J. Mol. Str. (THEOCHEM)* **528**, 193–198 (2000).
21. SYBYL6.5. (Tripos Associate, St. Louis (MO), 2000).
22. M.J.S. Dewar, E.G. Zoebisch, E.F. Healy and J.J.P. Stewart, *J. Am. Chem. Soc.* **107**, 3920 (1985).
23. A.D. Becke, *J. Chem. Phys.* **98**, 5648 (1993).
24. M.J. Frisch, G.W. Trucks, H.B. Schlegel, G.E. Scuseria, M.A. Robb, J.R. Cheeseman, Y.G. Zakrzewski, J.A. Montgomery, R.E. Stratmann, J.C. Burant, S. Dapprich, J.M. Millam, A.D. Daniels, K.N. Kudin, M.C. Strain, O. Farkas, J. Tomasi, Y. Barone, M. Cossi, R. Cammi, B. Mennucci, C. Pomelli, C. Adamo, S. Clifford, J. Ochterski, G.A. Petersson, P.Y. Ayala, Q. Cui, K. Morokuma, D.K. Malick, A.D. Rabuck, K. Raghavachari, J.B. Foresman, J. Cioslowski, J.V. Ortiz, B.B. Stefanov, G. Liu, A. Liashenko, P. Piskorz, I. Komaromi, R. Gomperts, R.L. Martin, D.J. Fox, T. Keith, M.A. Al-Laham, C.Y. Peng, A. Nanayakkara, C. Gonzalez, M. Challacombe, P.M.W. Gill, B.G. Johnson, W. Chen, M.W. Wong, J.L. Andres, M. Head-Gordon, E.S. Replogle and J.A. Pople, *Gaussian’98* (Gaussian Inc., Pittsburgh, PA, 1998).
25. WebLab<sup>TM</sup> (Molecular Simulation, Inc., San Diego, CA, 2000).
26. POV-ray<sup>©</sup> (POV-ray-Team1, POV-ray www.povray.org, 1998).
27. H. Dvir, M. Harel, H.L. Jiang, D.L. Bai, X.C. He, X.C. Tang, K.X. Chen, I. Silman and J.L. Sussman, unpublished result.
28. C.M. Breneman and K.B. Wiberg, *J. Comput. Chem.* **11**, 361–373 (1990).
29. J.L. Sussman, M. Harel, F. Frolow, C. Oefner, A. Goldman, L. Toker and I. Silman, *Science* **253**, 872–879 (1991).
30. A. Nicholls, K.A. Sharp and B. Honig, *Proteins* **11**, 281–296 (1991).
31. Y. Yamaguchi, M. Frisch, J. Gaw and H.F. Schaefer III, *J. Chem. Phys.* **84**, 2262–2278 (1986).
32. P. Pulay, G. Fogarasi, F.F. Pang and J.E. Boggs, *J. Am. Chem. Soc.* **101**, 2550–2560 (1979).
33. S.J. Geibuckmantel and A.P. Kozikowski, *Acta Cryst.* **C47**, 824–827 (1991).